Preformation probability inside α emitters having different ground state spin-parity than their daughters

W. M. Seif,* M. M. Botros, and A. I. Refaie
Faculty of Science, Department of Physics, Cairo University, Giza 12613, Egypt
(Received 23 July 2015; revised manuscript received 2 September 2015; published 5 October 2015)

The ground state spin and parity of a daughter formed in a radioactive α emitter are expected to influence the preformation probability of the α and daughter clusters inside it. We investigate the α and daughter preformation probability inside odd-A and doubly odd radioactive nuclei when the daughter and parent are of different spin and/or parity. We consider only the ground state to ground state unfavored decays. This is to extract precise information about the effect of the difference in the spin-parity of the ground states of the involved nuclei far away from any influence from the excitation energy, if the decays are coming from isomeric states. The calculations are done for 161 α emitters, with $65 \leqslant Z \leqslant 112$ and $84 \leqslant N \leqslant 173$, in the framework of the extended cluster model, with the Wentzel-Kramers-Brillouin penetrability and assault frequency. We used a Hamiltonian energy density scheme based on the Skyrme SLy4 interaction to compute the interaction potential. The α-plus-cluster preformation probability is extracted from the calculated decay width and the experimental half-life time. We discussed in detailed steps the effect of the angular momentum of the emitted α particle on the various physical quantities involved in the unfavored decay process and how it finally increases the half-life time. We found that if the ground state spin and/or parity of parent and daughter nuclei are different, then the preformation probability of the α cluster inside the parent is less than it would be if they had similar spin-parity. We modified the formula that gives the α preformation probability in terms of the numbers of protons and neutrons outside the shell closures of the parent, to account for this hindrance in the preformation probability for the unfavored decays between ground states.

DOI: 10.1103/PhysRevC.92.044302 PACS number(s): 23.60.+e, 21.60.Gx, 21.30.Fe, 27.90.+b

I. INTRODUCTION

In principle, the preformation probability of an emitted cluster inside a superheavy nucleus is one of the essential factors in predicting its dominant decay channel. Other factors are the released energy and the penetration probability. The uncertainties pertaining to the obtained values of the α-cluster preformation probability, or the α spectroscopic factor [1–3], in the different studies [4–8] make it one of the open problems in nuclear physics. The accurate determination of the preformation probability would help in estimating the half-life times of the superheavy elements, suggested to be synthesized in future, against their α decay modes. However, there are many confirmed factors which affect the α-cluster preformation probability. One of these factors is the deformation of the daughter that is formed in addition to the α cluster in the decaying nucleus, just before the decay process. The effect of the daughter deformation is found to decrease the preformation probability [7]. A second factor is the shell effect. As a function of the charge and neutron numbers, general oscillating patterns of the α preformation probability are observed with several local maxima and minima. While local minima are observed at the proton and neutron shell and subshell closures, the coexisting maxima are predicted around mid-shell occupation numbers of the proton and neutron open shells. The third affecting factor is the isospin asymmetry of the parent nucleus [3]. It is clarified that the preformation probability increases with increasing isospin asymmetry of the α emitters, if they have valence protons and neutrons but not holes. In the case of neutron or proton holes coexisting with the valence holes, the preformation probability decreases upon increasing the isospin asymmetry. The preformation probability is shown to exhibit individual linear behaviors as a function of the isospin asymmetry parameter multiplied by the valence proton and neutron numbers. The linear behaviors obtained are correlated with the shell closures in the parent nuclei [3]. Also, the existence of unpaired nucleons in the open shells of a parent nucleus influences the preformation process. This is the fourth affecting factor. Generally, the largest preformation probability of the α cluster inside a parent is assigned for spherical even (Z)–even (N) α emitters, which have no unpaired nucleons. The α preformation probability in decaying nuclei which have unpaired nucleons is shown to be less than it would be in their even-even neighboring isotopes, and isotones, with the same shell and subshell closures [9]. The effect of an unpaired neutron in hindering the preformation probability inside even-odd emitters appears to be slightly larger than that of the unpaired proton inside odd-even nuclei. The smallest α preformation probability is predicted inside deformed odd-odd decaying nuclei, which have an unpaired neutron and an unpaired proton at the same time.

Various approaches have been used to calculate the preformation probability. For instance, it can be calculated from the probability amplitude of the amount of α and daughter clustering inside the parent nucleus [4], or from the formation energy of the α cluster extracted from the binding energy differences of the involved nuclei [10]. To calculate the formation amplitude and the α decay probability by applying the R-matrix approach, the Skyrme-Hartree-Fock-Bogoliubov

*wseif@sci.cu.edu.eg

wave functions have been used in several studies [11]. Also, the α particle formation probabilities are deduced using the universal decay law method based on the R matrix [6]. Furthermore, they can be extracted from their explicit relation to the experimental half-life time [2,3,12] and the calculated decay width.

Concerning the unfavored decay process, one of the major consequences of the difference between the ground state spin-parity of parent and daughter is the angular momentum carried away by the emitted α particle. Indeed, the general trend of increasing the half-life time for such unfavored α decays due to the angular momentum transferred by the emitted α particle is considered in several studies [13,14]. Now, the pivotal question arises as to whether the preformation of the α plus daughter clusters has an independent probability regardless of the ground state spin-parity (J^π) of the parent and daughter. That is to say, if the parent and the formed daughter are of different spin-parity ground states, will the preformation probability be influenced? We want to consider this question in the present work.

We organize the paper as follows. In the next section, the theoretical approach for extracting and investigating the α preformation probability is outlined. The results for the studied nuclei are discussed in Sec. III. Finally, Sec. IV presents a brief summary and conclusion.

II. THEORETICAL FORMALISM

In the preformed cluster approaches [15,16], the partial half-life time ($T_{1/2}$) for a specific decay mode of an α emitter in a given spin (J)–parity (π) ground state (J^π_P) leaving a daughter in a state (J^π_D) is given as

$$T_{1/2}(\alpha) = \frac{\hbar \ln 2}{S_\alpha \Gamma_\alpha}. \tag{1}$$

Here, S_α denotes the preformation probability of the α and daughter as two individual clusters inside the decaying parent nucleus. Γ is the decay width. For the decays involving deformed daughter nuclei, the decay width at a given orientation angle (θ) reads

$$\Gamma(\theta) = \hbar \nu(\theta) P(\theta). \tag{2}$$

θ is usually defined as the relative angle between the separation vector $\vec{r}$ joining the centers of mass of α and daughter and the symmetry axis of the deformed daughter. In the framework of the well-known Wentzel-Kramers-Brillouin (WKB) approach, the tunneling assault frequency [$\nu(\theta)$] and penetration probability [$P(\theta)$] of the emitted α particle at a certain orientation θ are given, respectively, as

$$\nu(\theta) = T^{-1}(\theta) = \left[\int_{R_1(\theta)}^{R_2(\theta)} \frac{2\mu}{\hbar k(r,\theta)} dr \right]^{-1} \tag{3}$$

and

$$P(\theta) = e^{-2\int_{R_2(\theta)}^{R_3(\theta)} k(r,\theta) dr}. \tag{4}$$

In terms of the reduced mass of the α (m_α)-daughter (m_D) system [$\mu = m_\alpha m_D/(m_\alpha + m_D)$] and the experimental Q value [Q_α (MeV)] of the decay [17], the wave number $k(r,\theta)$ reads

$$k(r,\theta) = \sqrt{\frac{2\mu}{\hbar^2} |V_T(r,\theta) - Q_\alpha|}. \tag{5}$$

Along the oscillating and tunneling path of the α particle, the three classical turning points $R_{i=1,2,3}$ (fm) satisfy the condition $V_T(r,\theta)|_{r=R_i(\theta)} = Q_\alpha$. While the first two turning points [$R_{1,2}(\theta)$] depend on the emitting orientation, R_3 is independent of it [9]. Three contributions form the total real interaction potential [$V_T(r,\theta)$] between the two interaction clusters inside and outside the parent nucleus. Namely, they are the nuclear [$V_N(r,\theta)$], Coulomb [$V_C(r,\theta)$], and centrifugal [$V_\ell(r)$] parts,

$$V_T(r,\theta) = V_N(r,\theta) + V_C(r,\theta) + V_\ell(r). \tag{6}$$

We shall use the energy density formalism [18], with the frozen density approximation, to calculate the nuclear interaction part in terms of an appropriate Skyrme interaction [19–21],

$$V_N(r,\theta) = \int \{H[\rho_{p\alpha}(\vec{x}) + \rho_{pD}(r,\vec{x},\theta),\ \rho_{n\alpha}(\vec{x}) + \rho_{nD}(r,\vec{x},\theta)] - H_\alpha[\rho_{p\alpha}(\vec{x}),\ \rho_{n\alpha}(\vec{x})] - H_D[\rho_{pD}(\vec{x}),\ \rho_{nD}(\vec{x})]\} d\vec{x}. \tag{7}$$

The Skyrme energy-density functionals of the whole system (H), $\alpha(H_\alpha)$, and daughter (H_D) are given as functions of the proton (p) and neutron (n) frozen density distributions in the α and daughter clusters, $\rho_{ij}(i = p,n \text{ and } j = \alpha, D)$. The proton and neutron density distributions of the deformed nuclei are used in their two-parameter Fermi shape with radii and diffuseness parameters adjusted to reproduce the density distributions obtained from the self-consistent Hartree-Fock calculations [9]. The quadrupole (β_2), octupole (β_3), hexadecapole (β_4), and hexacontatetrapole (β_6) deformations [22] are expressed in the half-density radii of the Fermi density function. The SLy4 parametrization of the Skyrme-like nucleon-nucleon (NN) force [23] is used in the present calculations. The Skyrme-like force has the advantage of including explicitly the pairing and shell effect influences in the calculations [9]. The nuclear part of the interaction potential is usually normalized with a factor λ by applying the Bohr-Sommerfeld quantization condition [24] to ensure a quasistationary state [25]. For the potentials characterized by no repulsive core, such as the folding potentials based on the M3Y Reid and Paris NN interactions, this renormalization factor is very important for forming the internal pocket of the interaction potential. The Bohr-Sommerfeld condition is usually applied in terms of a global quantum number linked to the shell model through the Wildermuth quantization condition [12,14]. By applying the quantization condition for the nuclear part of the Skyrme-SLy4 interaction potential, without the kinetic energy part, a renormalization factor of value $\lambda \approx 0.510-0.640$ is obtained. This leads to volume integrals of the nuclear potential, per interacting nucleon pair, of about $J_R \approx 270-340\,\text{MeV fm}^3$, with a negative sign. Different studies have shown that the various α-nucleus potentials have volume integrals around $300 \pm 50\,\text{MeV fm}^3$, (Refs. [3,12] and the references therein). Fortunately, by including the kinetic energy part of the

energy density functional $H(\rho)$ of the Skyrme interaction, the quantization condition is verified automatically [3]. The Coulomb interaction $[V_C(r,\theta)]$ is also calculated based on the direct and exchange Coulomb functionals [26],

$$H_{\rm Coul}(\rho_p) = H_C^{\rm dir}(\rho_p) + H_C^{\rm exch}(\rho_p) = \frac{e^2}{2}\rho_p(\vec{r})\int \frac{\rho_p(\vec{r}')}{|\vec{r}-\vec{r}'|}d\vec{r}' - \frac{3e^2}{4}\left(\frac{3}{\pi}\right)^{1/3}[\rho_p(\vec{r})]^{4/3}. \quad (8)$$

To simplify the complications coming from the finite range of the proton-proton Coulomb force, the density multipole expansion of the deformed daughter has been used to calculate the Coulomb direct part [27,28]. If the ground state spin-parity of parent (J_P^π) and daughter (J_D^π) are not identical, we have then an unfavored decay mode. In such cases, the centrifugal potential part reads

$$V_\ell(r) = \frac{\ell(\ell+1)\hbar^2}{2\mu r^2}. \quad (9)$$

ℓ stands here for the angular momentum transferred by the emitted α particle, to conserve the spin and parity in the decay process. As the ground state spin-parity of the α particle is 0^+, the spin and parity conservation laws for the decay yield

$$|J_P - J_D| \leqslant \ell \leqslant |J_P + J_D| \quad (10)$$

and

$$\pi_P = \pi_D(-1)^\ell. \quad (11)$$

According to the principle of least action, we shall consider the minimum value of ℓ verifying Eqs. (10) and (11) as the preferred angular momentum carried out by the α particle. In this sense, $\ell_{\rm min}$ will be fixed as the minimum even (odd) value of ℓ from Eq. (10) if π_P and π_D are similar (different). However, by orientation averaging we obtain the average decay width as

$$\Gamma = \frac{1}{2}\int_0^\pi \Gamma(\theta)\sin\theta\, d\theta. \quad (12)$$

Based on its observed behavior with Z and N, a semiempirical formula was proposed [7,9] to give the α preformation probability in terms of the numbers of protons $(Z - Z_0)$ and neutrons $(N - N_0)$ outside the shell and subshell closures (Z_0, N_0) in the α emitter,

$$S_\alpha = Ae^{-\alpha(Z-Z_0-Z_c)^2}e^{-\beta(N-N_0-N_c)^2} - a_p,$$
$$a_p = \begin{cases} 0.0040\,(Z-Z_0)^{1/3} & \text{for odd } (Z) - \text{even } (N) \text{ nuclei,} \\ 0.0056\,(N-N_0)^{1/3} & \text{for even } (Z) - \text{odd } (N) \text{ nuclei,} \\ 0.0088\,(Z-Z_0+N-N_0)^{1/3} & \text{for odd } (Z) - \text{odd } (N) \text{ nuclei.} \end{cases} \quad (13)$$

Here Z_c (N_c) represents the number of protons (neutrons), outside the Z_0 (N_0) shell closures, which yields a local maximum value for the preformation probability. A, α, and β are dimensionless parameters, given below in Table III. The pairing term (a_p) takes account of the influences of the unpaired nucleon(s), inside the odd-A and odd (Z)-odd (N) α emitters, on the α-preformation probability [9].

III. RESULTS AND DISCUSSION

As mentioned above, our study is confined to the ground state to ground state decays to scrutinize only the effect of the difference in the ground state spin-parity, excluding any other effects due the excitation energy for the decays from isomeric states. The decays from 161 open-shell odd-A and odd (Z)—odd (N) radioactive α emitters in the mass region of $A = 149-285$ are mentioned. In Table I we list related structure information on the investigated α decays and the deduced preformation probabilities, $S_\alpha^{\rm expt} = \hbar \ln 2/\Gamma\, T_{1/2}^{\rm expt}$, Eq. (1). The experimental errors in both the Q value [17], column 6, and the experimental half-lives [29–36], column 7, are taken into account in deducing the preformation probability. The missing uncertainties of $S_\alpha^{\rm expt}$, in the eighth column, are of order 10^{-5} or less. The first five columns of Table I identify, respectively, the parent and daughter nuclei, and their ground state spin and parity ($J^\pi_{P(D)}$) in addition to the considered value of minimum angular momentum carried out by the emitted α particle ($\ell_{\rm min}$). Presented in the ninth and tenth columns, respectively, are the estimated preformation probabilities using the modified semiempirical formula given by Eq. (14), mentioned below, and the half-life times as obtained based on these values. Table I shows that only seven nuclei (≈4%) out of the 161 investigated α emitters yield a preformation probability greater than 0.1. The predicted value of $S_\alpha^{\rm expt}$ is in the order of 10^{-2} and 10^{-3} for 71 (≈44%) and 60 (≈37%) nuclei, respectively. Twenty-two studied cases (≈14%) yield a smaller $S_\alpha^{\rm expt}$ in the order of 10^{-4}. The α preformation probability in one of the investigated emitters (^{244}Bk) is obtained with a value less than 0.0001. In a similar study performed on the favored decays of 105 odd-A and odd (Z)-odd (N) nuclei [9], 6%, 80%, 13%, and only one nucleus among the investigated nuclei yielded α preformation probabilities in the order of 10^{-1}, 10^{-2}, 10^{-3}, and 10^{-4}, respectively. A larger relative number of α emitters (25%) yielding preformation probability greater than 0.1 is obtained for the even-even nuclei studied in Ref. [7]. The average α preformation probability inside all odd-even, even-odd, and odd-odd parent nuclei participating in the unfavored decays mentioned in the present work are 0.0242, 0.0303, and 0.0161, respectively. The corresponding average values inside the parent nuclei involved in the favored

TABLE I. The estimated α preformation probability S_α^{expt} [Eq. (1)], in the mentioned parent nuclei based on the experimental partial half-lives [$T_{1/2}^{\text{expt}}$ (s)] [29–36]. The uncertainties in the experimental half-life time and the intensity of the decay mode are both considered in the listed partial half-lives. The decay width is calculated using the WKB penetration probability and assault frequency, based on the Skyrme-SLy4 NN interaction. The first six columns identify, respectively, the parent (Pare.) and daughter (Dau.) nuclei, their ground state spin and parity ($J^\pi_{P(D)}$), the minimum expected value of the angular momentum carried out by the emitted α particle ($\ell_{\min}$), and the energy released through the decay process (Q_α values) [17]. The nonexperimental estimated spin and/or parity and their uncertain values are indicated in square brackets and parentheses [29], respectively. The last two columns exhibit the estimated preformation probability from the formula given by Eq. (14) and the calculated partial half-lives based on these values, respectively.

Pare.	Dau.	J_P^π	J_D^π	$\ell_{\min}$	Q_α (MeV)	$T_{1/2}^{\text{expt}}$ (s)	S_α^{expt} [Eq. (1)]	S_α [Eq. (14)]	$T_{1/2}^{\text{cal}}$ (s) [using S_α (Eq. (14)]
^{149}Tb	^{145}Eu	$1/2^+$	$5/2^+$	2	4.078 ± 0.002	$(8.976 \pm 0.968)\times10^{4}$	0.0311 ± 0.0044	0.0650	$4.315^{+0.055}_{-0.232}\times10^{4}$
^{151}Tb	^{147}Eu	$1/2^{(+)}$	$5/2^+$	2	3.497 ± 0.004	$(6.844 \pm 1.081)\times10^{8}$	0.0526 ± 0.0125	0.0660	$5.176^{+0.514}_{-0.358}\times10^{8}$
^{173}Hg	^{169}Pt	$[3/2^-]$	$(7/2^-)$	2	7.378 ± 0.004	$(9.100 \pm 2.600)\times10^{-4}$	0.1164 ± 0.0365	0.0181	$54.330^{+0.452}_{-2.767}\times10^{-4}$
^{177}Hg	^{173}Pt	$(7/2^-)$	$(5/2^-)$	2	6.740 ± 0.050	$(1.498 \pm 0.021)\times10^{-1}$	0.0709 ± 0.0294	0.0117	$8.241^{+4.463}_{-2.833}\times10^{-1}$
^{181}Hg	^{177}Pt	$1/2^{[-]}$	$5/2^-$	2	6.284 ± 0.004	13.434 ± 1.366	0.0143 ± 0.0022	0.0053	$35.161^{+2.320}_{-1.339}$
^{180}Tl	^{176}Au	$4^{(-)}$	(5^-)	2	6.710 ± 0.050	32.900 ± 22.100	0.0024 ± 0.0021	0.0041	$6.117^{+5.777}_{-1.090}$
^{179}Pb	^{175}Hg	$(9/2^-)$	$(7/2^-)$	2	7.598 ± 0.020	$3.500^{+1.400}_{-0.800}\times10^{-3}$ [31]	0.0230 ± 0.0096	0.0073	$10.503^{+1.630}_{-1.403}\times10^{-3}$
^{181}Pb	^{177}Hg	$(9/2^-)$	$(7/2^-)$	2	7.240 ± 0.007	$(3.900 \pm 0.080)\times10^{-2}$	0.0259 ± 0.0019	0.0049	$20.414^{+1.158}_{-1.056}\times10^{-2}$
^{183}Pb	^{179}Hg	$3/2^-$	$7/2^-$	2	6.928 ± 0.007	0.535 ± 0.030	0.0237 ± 0.0028	0.0028	$4.476^{+0.311}_{-0.272}$
^{185}Pb	^{181}Hg	$3/2^-$	$1/2^{[-]}$	2	6.695 ± 0.005	6.300 ± 0.400	0.0107 ± 0.0011	0.0053	$12.582^{+0.480}_{-0.574}$
^{187}Pb	^{183}Hg	$3/2^-$	$1/2^-$	2	6.393 ± 0.006	$(1.681 \pm 0.386)\times10^{2}$	0.0057 ± 0.0016	0.0063	$1.428^{+0.094}_{-0.077}\times10^{2}$
^{189}Pb	^{185}Hg	$3/2^-$	$1/2^-$	2	5.870 ± 0.040	$(1.263 \pm 0.053)\times10^{4}$	0.0136 ± 0.0062	0.0073	$2.061^{+1.221}_{-0.713}\times10^{4}$
^{184}Bi	^{180}Tl	$[3^+]$	$4^{(-)}$	1	8.020 ± 0.050	$(6.600 \pm 1.500)\times10^{-3}$	0.0011 ± 0.0006	0.0003	$17.985^{+7.247}_{-4.998}\times10^{-3}$
^{186}Bi	^{182}Tl	(3^+)	(7^+)	4	7.757 ± 0.012	$(1.480 \pm 0.070)\times10^{-2}$	0.0167 ± 0.0022	0.0105	$2.344^{+0.213}_{-0.193}\times10^{-2}$
^{187}Bi	^{183}Tl	$[9/2^-]$	$1/2^{(+)}$	5	7.779 ± 0.004	0.037 ± 0.002	0.0168 ± 0.0014	0.0256	$0.024^{+0.001}_{-0.001}$
^{188}Bi	^{184}Tl	$[3^+]$	$[2^-]$	1	7.264 ± 0.005	$(6.120 \pm 0.270)\times10^{-2}$	0.0202 ± 0.0013	0.0028	$43.420^{+0.917}_{-0.705}\times10^{-2}$
^{189}Bi	^{185}Tl	$(9/2^-)$	$[1/2^+]$	5	7.268 ± 0.003	0.658 ± 0.047	0.0415 ± 0.0039	0.0297	$0.918^{+0.019}_{-0.024}$
^{190}Bi	^{186}Tl	(3^+)	(2^-)	1	6.863 ± 0.004	6.300 ± 0.100	0.0046 ± 0.0002	0.0034	$8.357^{+0.285}_{-0.044}$
^{191}Bi	^{187}Tl	$(9/2^-)$	$(1/2^+)$	5	6.778 ± 0.003	25.406 ± 5.570	0.0639 ± 0.0159	0.0326	$46.587^{+1.962}_{-1.042}$
^{192}Bi	^{188}Tl	(3^+)	(2^-).	1	6.376 ± 0.005	$(3.527 \pm 1.545)\times10^{2}$	0.0077 ± 0.0036	0.0040	$5.425^{+0.238}_{-0.248}\times10^{2}$
^{193}Bi	^{189}Tl	$(9/2^-)$	$(1/2^+)$	5	6.304 ± 0.005	$(2.271 \pm 1.059)\times10^{3}$	0.0705 ± 0.0356	0.0342	$3.575^{+0.187}_{-0.173}\times10^{3}$
^{194}Bi	^{190}Tl	(3^+)	$2^{(-)}$	1	5.918 ± 0.005	$(2.981 \pm 1.685)\times10^{4}$	0.0104 ± 0.0062	0.0043	$4.778^{+0.267}_{-0.190}\times10^{4}$
^{195}Bi	^{191}Tl	$(9/2^-)$	$(1/2^+)$	5	5.832 ± 0.005	$(1.114 \pm 0.756)\times10^{6}$	0.0249 ± 0.0178	0.0342	$0.414^{+0.033}_{-0.025}\times10^{6}$
^{196}Bi	^{192}Tl	(3^+)	$2^{(-)}$	1	5.440 ± 0.040	$(2.950 \pm 0.976)\times10^{7}$	0.0023 ± 0.0015	0.0043	$1.049^{+0.683}_{-0.390}\times10^{7}$
^{209}Bi	^{205}Tl	$9/2^-$	$1/2^+$	5	3.137 ± 0.001	$(6.280 \pm 0.221)\times10^{26}$	0.0031 ± 0.0002	0.0120	$1.640^{+0.023}_{-0.053}\times10^{26}$
^{211}Bi	^{207}Tl	$9/2^-$	$1/2^+$	5	6.750 ± 0.001	128.400 ± 1.200	0.0045 ± 0.0001	0.0154	$37.833^{+0.189}_{-0.221}$
^{212}Bi	^{208}Tl	$1^{(-)}$	5^+	5	6.207	$(1.011 \pm 0.003)\times10^{4}$	0.0093	0.0133	0.708×10^{4}
^{213}Bi	^{209}Tl	$9/2^-$	$(1/2^+)$	5	5.982 ± 0.006	$(1.309 \pm 0.021)\times10^{5}$	0.0069 ± 0.0005	0.0186	$0.485^{+0.030}_{-0.029}\times10^{5}$
^{189}Po	^{185}Pb	$(5/2^-)$	$3/2^-$	2	7.694 ± 0.015	$(3.800 \pm 0.400)\times10^{-3}$	0.0691 ± 0.0146	0.0071	$36.011^{+4.163}_{-3.697}\times10^{-3}$
^{203}Po	^{199}Pb	$5/2^-$	$3/2^-$	2	5.496 ± 0.005	$(2.075 \pm 0.405)\times10^{6}$	0.0588 ± 0.0160	0.0071	$15.914^{+1.677}_{-0.959}\times10^{6}$
^{209}Po	^{205}Pb	$1/2^-$	$5/2^-$	2	4.979 ± 0.001	$(3.219 \pm 0.158)\times10^{9}$	0.0222 ± 0.0013	0.0024	$29.434^{+0.326}_{-0.318}\times10^{9}$
^{211}Po	^{207}Pb	$(9/2^+)$	$1/2^-$	5	7.595 ± 0.001	0.516 ± 0.003	0.0033	0.0140	$0.121^{+0.000}_{-0.001}$
^{194}At	^{190}Bi	$(4^-,5^-)$	(3^+)	1	7.462 ± 0.015	0.253 ± 0.010	0.0058 ± 0.0009	0.0044	$0.325^{+0.040}_{-0.034}$
^{195}At	^{191}Bi	$1/2^+$	$(9/2^-)$	5	7.339 ± 0.005	0.328 ± 0.020	0.2725 ± 0.0296	0.0347	$2.538^{+0.142}_{-0.103}$
^{210}At	^{206}Bi	$(5)^+$	$6^{(+)}$	2	5.631 ± 0.001	$(1.698 \pm 0.276)\times10^{7}$	0.0030 ± 0.0006	0.0009	$5.548^{+0.064}_{-0.163}\times10^{7}$
^{212}At	^{208}Bi	(1^-)	5^+	5	7.817 ± 0.001	0.314 ± 0.002	0.0027 ± 0.0001	0.0112	$0.075^{+0.001}_{-0.001}$
^{220}At	^{216}Bi	$3^{[-]}$	$(6^-,7^-)$	4	6.077 ± 0.018	$(2.976 \pm 0.774)\times10^{3}$	0.0935 ± 0.0421	0.0161	$14.441^{+4.138}_{-2.427}\times10^{3}$
^{193}Rn	^{189}Po	$[3/2^-]$	$(5/2^-)$	2	8.040 ± 0.012	$(1.150 \pm 0.270)\times10^{-3}$	0.0330 ± 0.0108	0.0091	$3.828^{+0.419}_{-0.354}\times10^{-3}$

TABLE I. (*Continued.*)

Pare.	Dau.	J_P^π	J_D^π	$\ell_{\min}$	Q_α (MeV)	$T_{1/2}^{\text{expt}}$ (s)	S_α^{expt} (Eq. (1))	S_α [Eq. (14)]	$T_{1/2}^{\text{cal}}$ (s) [using S_α (Eq. (14))]
^{205}Rn	^{201}Po	$5/2^-$	$3/2^-$	2	6.390 ± 0.050	$(6.918 \pm 0.424)\times10^{2}$	0.0960 ± 0.0488	0.0079	$77.117^{+41.839}_{-33.317}\times10^{2}$
^{211}Rn	^{207}Po	$1/2^-$	$5/2^-$	2	5.965 ± 0.001	$(1.927 \pm 0.146)\times10^{5}$	0.0178 ± 0.0016	0.0029	$11.749^{+0.253}_{-0.114}\times10^{5}$
^{213}Rn	^{209}Po	$[9/2^+]$	$1/2^-$	5	8.243 ± 0.005	$(1.950 \pm 0.010)\times10^{-2}$	0.0055 ± 0.0003	0.0150	$0.693^{+0.049}_{-0.015}\times10^{-2}$
^{219}Rn	^{215}Po	$5/2^+$	$9/2^+$	2	6.946	3.960 ± 0.010	0.0198 ± 0.0001	0.0097	8.112
^{221}Rn	^{217}Po	$7/2^+$	$(9/2^+)$	2	6.162 ± 0.002	$(7.030 \pm 0.456)\times10^{3}$	0.0118 ± 0.0010	0.0104	$8.000^{+0.125}_{-0.191}\times10^{3}$
^{210}Fr	^{206}At	6^+	$(5)^+$	2	6.672 ± 0.005	$(1.908 \pm 0.036)\times10^{2}$	0.0342 ± 0.0024	0.0029	$22.211^{+1.263}_{-1.009}\times10^{2}$
^{212}Fr	^{208}At	5^+	6^+	2	6.529 ± 0.002	$(1.200 \pm 0.036)\times10^{3}$	0.0242 ± 0.0013	0.0013	$22.762^{+0.680}_{-0.418}\times10^{3}$
^{214}Fr	^{210}At	$[1^-]$	$(5)^+$	5	8.589 ± 0.004	$(5.000 \pm 0.200)\times10^{-3}$	0.0051 ± 0.0002	0.0115	$2.218^{+0.018}_{-0.019}\times10^{-3}$
^{220}Fr	^{216}At	1^+	$1^{(-)}$	1	6.801 ± 0.002	27.400 ± 0.300	0.0296 ± 0.0008	0.0053	$156.792^{+0.304}_{-4.966}$
^{221}Fr	^{217}At	$5/2^-$	$9/2^-$	2	6.458 ± 0.001	286.620 ± 0.780	0.0425 ± 0.0007	0.0109	$1121.900^{+13.423}_{-17.376}$
^{207}Ra	^{203}Rn	$[5/2^-]$	$[3/2^-]$	2	7.270 ± 0.050	1.605 ± 0.209	0.0654 ± 0.0326	0.0085	$10.538^{+5.513}_{-3.551}$
^{213}Ra	^{209}Rn	$1/2^-$	$5/2^-$	2	6.862 ± 0.002	$(1.638 \pm 0.030)\times10^{2}$	0.0144 ± 0.0005	0.0032	$7.215^{+0.191}_{-0.025}\times10^{2}$
^{215}Ra	^{211}Rn	$[9/2^+]$	$1/2^-$	5	8.864 ± 0.003	$(1.670 \pm 0.010)\times10^{-3}$	0.0064 ± 0.0001	0.0158	$0.677^{+0.011}_{-0.010}\times10^{-3}$
^{219}Ra	^{215}Rn	$(7/2)^+$	$9/2^+$	2	8.138 ± 0.003	0.010 ± 0.003	0.0170 ± 0.0054	0.0092	$0.017^{+0.000}_{-0.001}$
^{221}Ra	^{217}Rn	$5/2^+$	$9/2^+$	2	6.880 ± 0.002	28.000 ± 2.000	0.0259 ± 0.0024	0.0104	$70.838^{+0.232}_{-2.684}$
^{223}Ra	^{219}Rn	$3/2^+$	$5/2^+$	2	5.979	$(98.755 \pm 0.432)\times10^{4}$	0.0017	0.0111	15.389×10^{4}
^{210}Ac	^{206}Fr	$[7^+]$	$(2^+,3^+)$	4	7.610 ± 0.050	0.350 ± 0.040	0.1806 ± 0.0862	0.0098	$5.594^{+2.810}_{-1.852}$
^{214}Ac	^{210}Fr	$[5^+]$	6^+	2	7.352 ± 0.003	8.200 ± 0.200	0.0129 ± 0.0006	0.0015	$69.508^{+1.311}_{-1.967}$
^{216}Ac	^{212}Fr	(1^-)	5^+	5	9.235 ± 0.006	$(4.400 \pm 0.160)\times10^{-4}$	0.0059 ± 0.0004	0.0116	$2.273^{+0.039}_{-0.121}\times10^{-4}$
^{220}Ac	^{216}Fr	(3^-)	(1^-)	2	8.348 ± 0.004	$(2.636 \pm 0.019)\times10^{-2}$	0.0014	0.0079	$0.480^{+0.015}_{-0.012}\times10^{-2}$
^{223}Ac	^{219}Fr	$(5/2^-)$	$9/2^-$	2	6.783 ± 0.001	127.273 ± 3.030	0.0176 ± 0.0007	0.0113	$197.258^{+3.077}_{-2.431}$
^{224}Ac	^{220}Fr	0^-	1^+	1	6.327 ± 0.001	$(1.113 \pm 0.266)\times10^{5}$	0.0008 ± 0.0002	0.0061	$0.143^{+0.001}_{-0.002}\times10^{5}$
^{225}Ac	^{221}Fr	$[3/2^-]$	$5/2^-$	2	5.935 ± 0.001	$(857.088 \pm 0.259)\times10^{3}$	0.0075 ± 0.0001	0.0119	$540.738^{+9.430}_{-8.475}\times10^{3}$
^{226}Ac	^{222}Fr	$(1)^{[-]}$	2^-	2	5.536 ± 0.021	$(1.985 \pm 0.669)\times10^{9}$	0.0003 ± 0.0002	0.0102	$0.048^{+0.015}_{-0.011}\times10^{9}$
^{209}Th	^{205}Ra	$[5/2^-]$	$(3/2^-)$	2	8.270 ± 0.050	$(3.100 \pm 1.200)\times10^{-3}$	0.0855 ± 0.0546	0.0089	$21.244^{+8.709}_{-6.324}\times10^{-3}$
^{211}Th	^{207}Ra	$[5/2^-]$	$[3/2^-]$	2	7.940 ± 0.050	0.048 ± 0.020	0.0761 ± 0.0480	0.0071	$0.338^{+0.153}_{-0.068}$
^{215}Th	^{211}Ra	$(1/2^-)$	$5/2^-$	2	7.665 ± 0.004	1.200 ± 0.200	0.0207 ± 0.0043	0.0035	$6.803^{+0.377}_{-0.184}$
^{217}Th	^{213}Ra	$[9/2^+]$	$1/2^-$	5	9.435 ± 0.004	$(2.470 \pm 0.040)\times10^{-4}$	0.0075 ± 0.0003	0.0161	$1.153^{+0.020}_{-0.024}\times10^{-4}$
^{221}Th	^{217}Ra	$(7/2^+)$	$(9/2^+)$	2	8.626 ± 0.004	$(1.680 \pm 0.060)\times10^{-3}$	0.0075 ± 0.0005	0.0096	$1.311^{+0.054}_{-0.031}\times10^{-3}$
^{223}Th	^{219}Ra	$(5/2)^+$	$(7/2)^+$	2	7.567 ± 0.004	0.600 ± 0.020	0.0129 ± 0.0008	0.0108	$0.716^{+0.022}_{-0.023}$
^{225}Th	^{221}Ra	$(3/2^+)$	$5/2^+$	2	6.921 ± 0.002	525.000 ± 2.400	0.0019	0.0116	$85.584^{+1.402}_{-1.627}$
^{227}Th	^{223}Ra	$1/2^+$	$3/2^+$	2	6.147	$(161.395 \pm 0.778)\times10^{4}$	0.0006	0.0118	7.803×10^{4}
^{229}Th	^{225}Ra	$5/2^+$	$1/2^+$	2	5.168 ± 0.001	$(2.503 \pm 0.017)\times10^{11}$	0.0007	0.0114	$0.161^{+0.002}_{-0.004}\times10^{11}$
^{224}Pa	^{220}Ac	$[5^-]$	(3^-)	2	7.694 ± 0.004	0.844 ± 0.019	0.0072 ± 0.0004	0.0093	$0.655^{+0.021}_{-0.020}$
^{225}Pa	^{221}Ac	$[5/2^-]$	$[9/2^-]$	2	7.390 ± 0.050	1.700 ± 0.200	0.0330 ± 0.0161	0.0115	$4.241^{+2.166}_{-1.454}$
^{228}Pa	^{224}Ac	3^+	0^-	3	6.265 ± 0.002	$(4.018 \pm 0.582)\times10^{6}$	0.0003	0.0144	$0.071^{+0.002}_{-0.001}\times10^{6}$
^{229}Pa	^{225}Ac	$(5/2^+)$	$[3/2^-]$	1	5.835 ± 0.004	$(2.739 \pm 0.375)\times10^{7}$	0.0022 ± 0.0004	0.0075	$0.765^{+0.041}_{-0.034}\times10^{7}$
^{230}Pa	^{226}Ac	(2^-)	$(1)^{[-]}$	2	5.439 ± 0.001	$(4.707 \pm 0.282)\times10^{10}$	0.0004	0.0100	$0.167^{+0.002}_{-0.002}\times10^{10}$
^{217}U	^{213}Th	$[1/2^-]$	$[5/2^-]$	2	8.430 ± 0.070	$0.016^{+0.021}_{-0.006}$ [30]	0.0413 ± 0.0336	0.0036	$0.129^{+0.081}_{-0.049}$
^{219}U	^{215}Th	$[9/2^+]$	$(1/2^-)$	5	9.940 ± 0.050	$(5.500 \pm 2.500)\times10^{-5}$	0.0145 ± 0.0094	0.0160	$3.379^{+1.091}_{-0.791}\times10^{-5}$
^{223}U	^{219}Th	$[7/2^+]$	$[9/2^+]$	2	8.940 ± 0.050	$(2.100 \pm 0.800)\times10^{-5}$	0.5986 ± 0.3679	0.0097	$94.670^{+35.152}_{-25.529}\times10^{-5}$
^{225}U	^{221}Th	$[5/2^+]$	$(7/2^+)$	2	8.015 ± 0.007	0.061 ± 0.004	0.0240 ± 0.0029	0.0109	$0.133^{+0.008}_{-0.007}$
^{227}U	^{223}Th	$(3/2^+)$	$(5/2)^+$	2	7.211 ± 0.014	66.000 ± 6.000	0.0048 ± 0.0010	0.0117	$26.775^{+3.244}_{-3.244}$
^{231}U	^{227}Th	$(5/2)^{[+]}$	$1/2^+$	2	5.576 ± 0.002	$(9.734 \pm 2.650)\times10^{9}$	0.0026 ± 0.0009	0.0116	$1.834^{+0.330}_{-0.068}\times10^{9}$

TABLE I. (*Continued.*)

Pare.	Dau.	J_P^π	J_D^π	$\ell_{\min}$	Q_α (MeV)	$T_{1/2}^{\text{expt}}$ (s)	S_α^{expt} [Eq. (1)]	S_α [Eq. (14)]	$T_{1/2}^{\text{cal}}$ (s) [using S_α (Eq. (14)]
^{235}U	^{231}Th	$7/2^-$	$5/2^+$	1	4.678 ± 0.001	$(2.221 \pm 0.002)\times10^{16}$	0.0003	0.0057	$0.116^{+0.002}_{-0.003}\times10^{16}$
^{227}Np	^{223}Pa	$[5/2^-]$	$[9/2^-]$	2	7.816 ± 0.014	0.510 ± 0.060	0.0147 ± 0.0033	0.0114	$0.634^{+0.076}_{-0.064}$
^{229}Np	^{225}Pa	$[5/2^+]$	$[5/2^-]$	1	7.010 ± 0.050	$(2.400 \pm 0.108)\times10^{2}$	0.0103 ± 0.0048	0.0074	$2.933^{+1.744}_{-1.072}\times10^{2}$
^{231}Np	^{227}Pa	$(5/2)^{[+]}$	$(5/2^-)$	1	6.370 ± 0.050	$(1.956 \pm 0.984)\times10^{5}$	0.0388 ± 0.0309	0.0075	$5.309^{+3.793}_{-2.197}\times10^{5}$
^{235}Np	^{231}Pa	$5/2^+$	$3/2^-$	1	$5.194 \pm 0.002.$	$(1.320 \pm 0.070)\times10^{12}$	0.0055 ± 0.0005	0.0064	$1.126^{+0.046}_{-0.025}\times10^{12}$
^{236}Np	^{232}Pa	(6^-)	(2^-)	4	5.010 ± 0.050	$(3.245 \pm 0.910)\times10^{15}$	0.0001 ± 0.0001	0.0135	$0.019^{+0.010}_{-0.011}\times10^{15}$
^{237}Np	^{233}Pa	$5/2^+$	$3/2^-$	1	4.959 ± 0.001	$(6.766 \pm 0.022)\times10^{13}$	0.0031	0.0055	$3.841^{+0.078}_{-0.005}\times10^{13}$
^{229}Pu	^{225}U.	$[3/2^+]$	$[5/2^+]$	2	7.590 ± 0.050	91.000 ± 26.000	0.0083 ± 0.0051	0.0116	$50.039^{+25.653}_{-17.556}$
^{233}Pu	^{229}U	$(5/2^+)$	$(3/2^+)$	2	6.420 ± 0.050	$(1.275 \pm 0.055)\times10^{6}.$	0.0067 ± 0.0035	0.0114	$0.634^{+0.449}_{-0.259}\times10^{6}$
^{237}Pu	^{233}U	$7/2^-$	$5/2^+$	1	5.748 ± 0.002	$(9.476 \pm 0.911)\times10^{10}$	0.0001	0.0057	$0.180^{+0.003}_{-0.005}\times10^{10}$
^{239}Pu	^{235}U	$1/2^+$	$7/2^-$	3	5.245	$(7.608 \pm 0.009)\times10^{11}$	0.0318	0.0101	23.904×10^{11}
^{241}Pu	^{237}U	$5/2^+$	$1/2^+$	2	5.140 ± 0.001	$(1.840 \pm 0.016)\times10^{13}$	0.0038 ± 0.0001	0.0057	$1.232^{+0.008}_{-0.033}\times10^{13}$
^{235}Am	^{231}Np	$[5/2^-]$	$(5/2)^{[+]}$	1	6.576 ± 0.013	$(1.400 \pm 0.236)\times10^{5}$ [32]	0.0189 ± 0.0057	0.0069	$3.596^{+0.545}_{-0.458}\times10^{5}$
^{239}Am	^{235}Np	$(5/2)^-$	$5/2^+$	1	5.922 ± 0.001	$(4.331 \pm 0.469)\times10^{8}$	0.0087 ± 0.0011	0.0053	$6.952^{+0.148}_{-0.101}\times10^{8}$
^{240}Am	^{236}Np	(3^-)	(6^-)	4	5.710 ± 0.050	$(1.116 \pm 0.417)\times10^{11}$	0.0012 ± 0.0009	0.0101	$0.076^{+0.074}_{-0.035}\times10^{11}$
^{241}Am	^{237}Np	$5/2^-$	$5/2^+$	1	5.638	$(1.365 \pm 0.002)\times10^{10}$	0.0105	0.0043	3.330×10^{10}
^{243}Am	^{239}Np	$5/2^-$	$5/2^+$	1	5.439 ± 0.001	$(2.326 \pm 0.013)\times10^{11}$	0.0086 ± 0.0002	0.0033	$6.045^{+0.116}_{-0.037}\times10^{11}$
^{239}Cm	^{235}Pu	$(7/2^-)$	$(5/2^+)$	1	6.540 ± 0.050	$(1.585 \pm 0.590)\times10^{8}$	0.0001 ± 0.0001	0.0055	$0.018^{+0.013}_{-0.008}\times10^{8}$
^{241}Cm	^{237}Pu	$1/2^+$	$7/2^-$	3	6.185 ± 0.001	$(2.864 \pm 0.304)\times10^{8}$	0.0048 ± 0.0006	0.0097	$1.400^{+0.028}_{-0.024}\times10^{8}$
^{243}Cm	^{239}Pu	$5/2^+$	$1/2^+$	2	6.169 ± 0.001	$(9.183 \pm 0.032)\times10^{8}$	0.0009	0.0055	$1.546^{+0.004}_{-0.007}\times10^{8}$
^{245}Cm	^{241}Pu	$7/2^+$	$5/2^+$	2	5.623 ± 0.001	$(2.658 \pm 0.023)\times10^{11}$	0.0033 ± 0.0001	0.0039	$2.290^{+0.009}_{-0.073}\times10^{11}$
^{247}Cm	^{243}Pu	$9/2^-$	$7/2^+$	1	5.354 ± 0.003	$(4.923 \pm 0.158)\times10^{14}$	0.0001	0.0017	$0.152^{+0.004}_{-0.008}\times10^{14}$
^{243}Bk	^{239}Am	$[3/2^-]$	$(5/2)^-$	2	6.874 ± 0.004	$(1.080 \pm 0.048)\times10^{7}$	0.0001	0.0065	$0.022^{+0.001}_{-0.001}\times10^{7}$
^{244}Bk	^{240}Am	$[4^-]$	(3^-)	2	6.779 ± 0.004	$(3.540 \pm 1.860)\times10^{8}$	0.00001 ± 0.00001	0.0038	0.008×10^{8}
^{245}Bk	^{241}Am	$3/2^-$	$5/2^-$	2	6.455 ± 0.001	$(3.591 \pm 0.321)\times10^{8}$	0.0002	0.0049	$0.155^{+0.000}_{-0.005}\times10^{8}$
^{247}Bk	^{243}Am	$(3/2^-)$	$5/2^-$	2	5.890 ± 0.005	$(4.355 \pm 0.789)\times10^{10}$	0.0019 ± 0.0005	0.0017	$4.854^{+0.294}_{-0.331}\times10^{10}$
^{249}Bk	^{245}Am	$7/2^+$	$(5/2)^+$	2	5.523 ± 0.002	$(1.974 \pm 0.133)\times10^{12}$	0.0055 ± 0.0005	0.0026	$4.148^{+0.092}_{-0.127}\times10^{12}$
^{237}Cf	^{233}Cm	$[5/2^+]$	$[3/2^+]$	2	8.220 ± 0.050	0.800 ± 0.200	0.0561 ± 0.0315	0.0103	$3.514^{+1.597}_{-1.127}$
^{247}Cf	^{243}Cm	$[7/2^+]$	$5/2^+$	2	6.495 ± 0.015	$(3.270 \pm 0.498)\times10^{7}$	0.0049 ± 0.0015	0.0036	$4.225^{+0.765}_{-0.622}\times10^{7}$
^{249}Cf	^{245}Cm	$9/2^-$	$7/2^+$	1	6.296 ± 0.001	$(1.108 \pm 0.006)\times10^{10}$	0.0001	0.0016	$0.075^{+0.001}_{-0.000}\times10^{10}$
^{251}Cf	^{247}Cm	$1/2^+$	$9/2^-$	5	6.177 ± 0.001	$(2.840 \pm 0.126)\times10^{10}$	0.0027 ± 0.0002	0.0067	$1.156^{+0.018}_{-0.012}\times10^{10}$
^{253}Cf	^{249}Cm	$(7/2^+)$	$[1/2^+]$	4	6.126 ± 0.004	$(5.051 \pm 0.674)\times10^{8}$	0.1017 ± 0.0158	0.0070	$72.715^{+1.309}_{-1.957}\times10^{8}$
^{245}Es	^{241}Bk	$(3/2^-)$	$(7/2^+)$	3	7.909 ± 0.003	$(1.800 \pm 0.600)\times10^{2}$	0.0096 ± 0.0034	0.0080	$1.907^{+0.045}_{-0.037}\times10^{2}$
^{246}Es	^{242}Bk	$[4^-]$	$[2^-]$	2	7.740 ± 0.100	$(4.758 \pm 1.168)\times10^{3}$	0.0013 ± 0.0010	0.0034	$1.048^{+1.414}_{-0.596}\times10^{3}$
^{252}Es	^{248}Bk	(4^+)	$[6^+]$	2	6.790 ± 0.050	$(4.075 \pm 0.016)\times10^{7}$	0.0007 ± 0.0003	0.0017	$1.550^{+0.983}_{-0.667}\times10^{7}$
^{254}Es	^{250}Bk	(7^+)	2^-	5	6.616 ± 0.002	$(2.382 \pm 0.004)\times10^{7}$	0.0596 ± 0.0013	0.0052	$27.470^{+0.424}_{-0.637}\times10^{7}$
^{255}Es	^{251}Bk	$(7/2^+)$	$(3/2^-)$	3	6.436 ± 0.001	$(4.316 \pm 0.345)\times10^{7}$	0.0420 ± 0.0036	0.0056	$32.031^{+0.018}_{-0.319}\times10^{7}$
^{243}Fm	^{239}Cf	$[7/2^-]$	$[5/2^+]$	1	8.690 ± 0.050	0.231 ± 0.009	0.0205 ± 0.0077	0.0047	$0.935^{+0.400}_{-0.282}$
^{245}Fm	^{241}Cf	$[1/2^+]$	$[7/2^-]$	3	8.440 ± 0.100	4.200 ± 1.300	0.0253 ± 0.0199	0.0082	$7.525^{+8.438}_{-3.937}$
^{247}Fm	^{243}Cf	$[7/2^+]$	$[1/2^+]$	4	8.258 ± 0.010	31.000 ± 1.000	0.0135 ± 0.0015	0.0079	$53.246^{+4.331}_{-4.204}$
^{249}Fm	^{245}Cf	$(7/2^+)$	$1/2^+$	4	7.709 ± 0.006	$(5.482 \pm 2.768)\times10^{2}$ [33]	0.0936 ± 0.0506	0.0054	$68.780^{+3.110}_{-3.579}\times10^{2}$
^{251}Fm	^{247}Cf	$(9/2^-)$	$[7/2^+]$	1	7.425 ± 0.002	$(1.066 \pm 0.087)\times10^{6}$	0.0001	0.0015	$0.062^{+0.001}_{-0.002}\times10^{6}$
^{253}Fm	^{249}Cf	$(1/2)^+$	$9/2^-$	5	7.198 ± 0.003	$(2.182 \pm 0.268)\times10^{6}$	0.0050 ± 0.0007	0.0061	$1.767^{+0.040}_{-0.046}\times10^{6}$
^{255}Fm	^{251}Cf	$7/2^+$	$1/2^+$	4	7.240 ± 0.002	$(7.225 \pm 0.025)\times10^{4}$	0.0362 ± 0.0008	0.0063	$42.000^{+0.238}_{-1.253}\times10^{4}$

TABLE I. (*Continued.*)

Pare.	Dau.	J_P^π	J_D^π	$\ell_{\min}$	Q_α (MeV)	$T_{1/2}^{\text{expt}}$ (s)	S_α^{expt} [Eq. (1)]	S_α [Eq. (14)]	$T_{1/2}^{\text{cal}}$ (s) [using S_α (Eq. (14)]
^{257}Fm	^{253}Cf	$(9/2^+)$	$(7/2^+)$	2	6.864 ± 0.001	$(8.683 \pm 0.017)\times 10^6$	0.0040 ± 0.0001	0.0045	$7.596^{+0.209}_{-0.002}\times 10^6$
^{247}Md	^{243}Es	$(7/2^-)$	$(7/2^+)$	1	8.764 ± 0.010	1.190 ± 0.090	0.0051 ± 0.0008	0.0033	$1.808^{+0.133}_{-0.132}$
^{249}Md	^{245}Es	$(7/2^-)$	$(3/2^-)$	2	8.441 ± 0.018	23.400 ± 2.400	0.0034 ± 0.0008	0.0039	$19.643^{+2.841}_{-2.402}$
^{251}Md	^{247}Es	$(7/2^-)$	$(7/2^+)$	1	7.963 ± 0.004	$(2.565 \pm 0.395)\times 10^3$	0.0009 ± 0.0002	0.0008	$3.021^{+0.078}_{-0.095}\times 10^3$
^{255}Md	^{251}Es	$(7/2^-)$	$(3/2^-)$	2	7.906 ± 0.003	$(2.200 \pm 0.700)\times 10^4$	0.0002 ± 0.0001	0.0029	$0.159^{+0.005}_{-0.005}\times 10^4$
^{256}Md	^{252}Es	(1^-)	(4^+)	3	7.856 ± 0.016 [34]	$(5.061 \pm 0.516)\times 10^4$ [34]	0.0003 ± 0.0001	0.0028	$0.449^{+0.071}_{-0.054}\times 10^4$
^{257}Md	^{253}Es	$(7/2^-)$	$7/2^+$	1	7.558 ± 0.001	$(1.383 \pm 0.289)\times 10^5$	0.0005 ± 0.0001	0.0024	$0.302^{+0.002}_{-0.000}\times 10^5$
^{258}Md	^{254}Es	(8^-)	(7^+)	1	7.271 ± 0.002	$(4.450 \pm 0.026)\times 10^6$	0.0003	0.0019	$0.610^{+0.010}_{-0.006}\times 10^6$
^{253}No	^{249}Fm	$(9/2^-)$	$(7/2^+)$	1	8.414 ± 0.004	93.600 ± 1.200	0.0018 ± 0.0001	0.0010	$169.264^{+6.118}_{-5.098}$
^{255}No	^{251}Fm	$(1/2^+)$	$(9/2^-)$	5	8.428 ± 0.003	$(2.112 \pm 0.108)\times 10^2$	0.0070 ± 0.0005	0.0040	$3.707^{+0.089}_{-0.081}\times 10^2$
^{257}No	^{253}Fm	$(7/2^+)$	$(1/2)^+$	4	8.477 ± 0.006	24.500 ± 0.500	0.0183 ± 0.0012	0.0042	$106.619^{+5.776}_{-3.610}$
^{259}No	^{255}Fm	$[9/2^+]$	$7/2^+$	2	7.858 ± 0.005 [35]	$(3.480 \pm 0.300)\times 10^3$ [35]	0.0069 ± 0.0009	0.0030	$7.834^{+0.332}_{-0.279}\times 10^3$
^{255}Lr	^{251}Md	$(1/2^-)$	$(7/2^-)$	4	8.556 ± 0.007	31.100 ± 1.100	0.0218 ± 0.0018	0.0035	$194.067^{+7.706}_{-9.989}$
^{257}Lr	^{253}Md	$(1/2^-)$	$(7/2^-)$	4	9.010 ± 0.030	6.000 ± 0.400	0.0036 ± 0.0009	0.0046	$4.404^{+0.978}_{-0.758}$
^{259}Lr	^{255}Md	$[1/2^-]$	$(7/2^-)$	4	8.580 ± 0.070	7.964 ± 0.589	0.0934 ± 0.0509	0.0058	$107.651^{+76.795}_{-44.551}$
^{255}Rf	^{251}No	$(9/2^-)$	$(7/2^+)$	1	9.055 ± 0.004	1.660 ± 0.070	0.0057 ± 0.0004	0.0012	$8.042^{+0.245}_{-0.216}$
^{257}Rf	^{253}No	$(1/2^+)$	$(9/2^-)$	5	9.083 ± 0.008	4.820 ± 0.130	0.0166 ± 0.0014	0.0047	$16.910^{+1.041}_{-0.962}$
^{259}Rf	^{255}No	$[7/2^+]$	$(1/2^+)$	4	9.130 ± 0.070	2.630 ± 0.260	0.0104 ± 0.0054	0.0050	$4.655^{+2.894}_{-1.759}$
^{261}Rf	^{257}No	$[3/2^+]$	$(7/2^+)$	2	8.650 ± 0.050	8.831 ± 3.074	0.0335 ± 0.0211	0.0036	$59.512^{+27.403}_{-18.546}$
^{257}Db	^{253}Lr	$(9/2^+)$	$(7/2^-)$	1	9.206 ± 0.020	2.300 ± 0.200	0.0034 ± 0.0008	0.0014	$5.361^{+0.734}_{-0.755}$
^{259}Db	^{255}Lr	$[9/2^+]$	$(1/2^-)$	5	9.620 ± 0.050	0.510 ± 0.160 [35]	0.0108 ± 0.0062	0.0061	$0.704^{+0.276}_{-0.193}$
^{259}Sg	^{255}Rf	$[1/2^+]$	$(9/2^-)$	5	9.804 ± 0.021	0.280 ± 0.050	0.0124 ± 0.0038	0.0054	$0.597^{+0.088}_{-0.075}$
^{261}Sg	^{257}Rf	$(3/2^+)$	$(1/2^+)$	2	9.714 ± 0.015	0.183 ± 0.005	0.0042 ± 0.0005	0.0034	$0.220^{+0.023}_{-0.019}$
^{265}Sg	^{261}Rf	$[9/2^+]$	$[3/2^+]$	4	8.823 ± 0.051 [36]	16.500 ± 5.500 [36]	0.1112 ± 0.0701	0.0078	$169.980^{+85.438}_{-54.055}$
^{261}Bh	^{257}Db	$(5/2^-)$	$(9/2^+)$	3	10.500 ± 0.050	$(1.28 \pm 0.320)\times 10^{-2}$	0.0021 ± 0.0010	0.0044	$0.500^{+0.167}_{-0.123}\times 10^{-2}$
^{263}Hs	^{259}Sg	$[7/2^+]$	$[1/2^+]$	4	10.730 ± 0.050	$(7.600 \pm 0.400)\times 10^{-4}$	0.0337 ± 0.0110	0.0063	$38.544^{+12.347}_{-98.178}\times 10^{-4}$
^{267}Hs	^{263}Sg	$[5/2^+]$	$[7/2^+]$	2	10.037 ± 0.013	$(5.500 \pm 1.100)\times 10^{-2}$	0.0097 ± 0.0027	0.0053	$9.581^{+0.754}_{-0.767}\times 10^{-2}$
^{267}Ds	^{263}Hs	$[9/2^+]$	$[7/2^+]$	2	11.780 ± 0.050	$(1.000 \pm 0.800)\times 10^{-5}$	0.0277 ± 0.0241	0.0050	$1.613^{+0.460}_{-0.337}\times 10^{-5}$
^{269}Ds	^{265}Hs	$[9/2^+]$	$[3/2^+]$	4	11.509 ± 0.030	$(2.300 \pm 1.100)\times 10^{-4}$	0.0073 ± 0.0043	0.0093	$1.279^{+0.217}_{-0.187}\times 10^{-4}$
^{271}Ds	^{267}Hs	$[13/2^-]$	$[5/2^+]$	5	10.870 ± 0.018	0.090 ± 0.040	0.0018 ± 0.0009	0.0120	$0.010^{+0.001}_{-0.001}$
^{273}Ds	^{269}Hs	$[13/2^-]$	$[9/2^+]$	3	11.370 ± 0.050	$(2.400 \pm 1.200)\times 10^{-4}$	0.0102 ± 0.0069	0.0084	$1.872^{+0.577}_{-0.431}\times 10^{-4}$
^{277}Ds	^{273}Hs	$[11/2^+]$	$[3/2^+]$	4	10.840 ± 0.110	0.022 ± 0.017	0.0098 ± 0.0091	0.0092	$0.006^{+0.005}_{-0.003}$
^{277}Cn	^{273}Ds	$[3/2^+]$	$[13/2^-]$	5	11.620 ± 0.050	$(9.900 \pm 4.900)\times 10^{-4}$	0.0128 ± 0.0085	0.0125	$6.520^{+2.007}_{-1.488}\times 10^{-4}$
^{281}Cn	^{277}Ds	$[3/2^+]$	$[11/2^+]$	4	10.460 ± 0.050	0.370 ± 0.290	0.0289 ± 0.0253	0.0084	$0.378^{+0.137}_{-0.100}$
^{285}Cn	^{281}Ds	$[5/2^+]$	$[3/2^+]$	2	9.320 ± 0.050	32.000 ± 9.000	0.1068 ± 0.0618	0.0033	$831.107^{+346.168}_{-271.468}$

decays mentioned in Ref. [9] are 0.0446, 0.0361, and 0.0322, respectively. However, the preformation probability inside odd-A and odd-odd nuclei exhibits relatively smaller values for unfavored decays with respect to the favored ones.

In addition to an expected change in the α preformation probability involved in the unfavored decays, the nonzero angular momentum carried by the emitted α particle impacts the different parameters and quantities participating in the decay process. As example, we present in Fig. 1 the orientation and the ℓ dependence of the total interaction potential, Eqs. (6)–(9), of $\alpha + {}^{251}$Cf ($\beta_2 = 0.236$, $\beta_4 = 0.024$, and $\beta_6 = -0.037$ [22]), which controls the α-decay process of ^{255}Fm ($Q_\alpha = 7.240$ MeV). Figure 1 shows that, for $\ell = 0$, the positions of the first two turning points change from $R_1 = 7.82$ fm and $R_2 = 9.64$ fm at the orientation $\theta = 0^\circ$ to $R_1 = 7.02$ fm and $R_2 = 7.80$ fm at $\theta = 90^\circ$. The position of the third turning point is fixed at $R_3 = 38.98$ fm for the two mentioned orientations. With increasing ℓ, the positions of

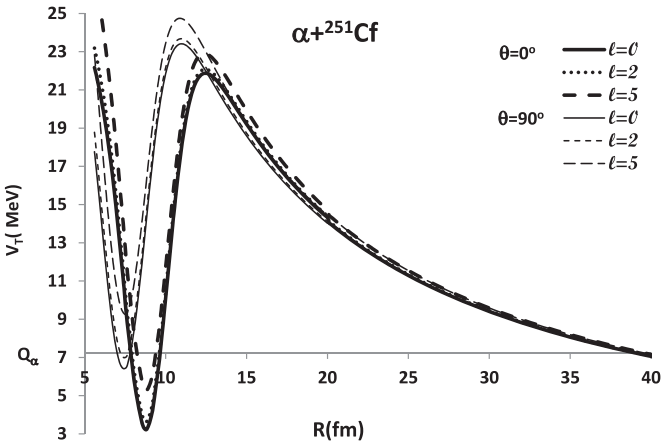

FIG. 1. The orientation and the ℓ dependence of the total interaction potential, Eqs. (6)–(9), between α particle and ^{251}Cf nucleus. The nuclear part is computed in terms of the Skyrme-SLy4 effective NN interaction.

R_1 and R_3 shift to larger internuclear distances, between the two interacting nuclei, while R_2 shifts to less distance. The exact folding calculations of the Coulomb interaction part, Eq. (8), yield an accurate total interaction potential. The widely used approximate formulas which consider interacting homogeneous charged spheres produce large errors in the overlap and surface regions of the interaction potential [37]. At some orientations, this error exceeds 100% (50%) in the overlap (surface) region at which the R_1 (R_2) critical turning point takes place. The approximate formulas do not affect R_3 seriously. However, Fig. 1 and our detailed results show that, as ℓ increases, the width of the internal pocket of the total interaction potential ($R_2 - R_1$) decreases and its lowest point shifts up. These two factors increase the assault frequency. On the other hand, the increasing of ℓ produces a higher Coulomb barrier characterized by a wider barrier width, $R_3 - R_2$. Also, the radius of the Coulomb barrier slightly decreases. Subsequently, the penetration probability decreases. The relative reduction in the penetration probability due to the nonzero ℓ is more prominent, in the decay process, than the increase in the assault frequency. Consequently, the net effect of these two opposite factors is to reduce the decay width. However, the overall impact of the nonzero transferred angular momentum on the unfavored decay mode appears as a substantial increase in half-life time. Of course, the presence of barrier distribution due to any deformation in the involved nuclei increases the range of variation of all mentioned quantities, and consequently the effect of ℓ appears more clearly.

Displayed in Fig. 2 are the estimated α-preformation probability in the even-odd isotopes of Rn ($Z = 86$) and Cm ($Z = 96$), the odd-even isotopes of Ac ($Z = 89$) and Pa ($Z = 91$), and the odd-odd ones of At ($Z = 85$) and Pa ($Z = 91$), as a function of the neutron number of the α emitters. In this figure, the present results for the unfavored decays with $\ell_{\min} \neq 0$ (open symbols) are compared with those of the favored decays with $\ell_{\min} = 0$ (solid symbols) for the same mentioned isotopic chains, taken from Ref. [9]. Generally, the presented results follow the oscillatory behavior detected for S_α as a function of N [7]. The average S_α^{expt} for the shown unfavored decays involving odd-even, even-odd, and odd-odd nuclei are 0.0151, 0.0176, and 0.0161, respectively. The corresponding values for the displayed favored decays are, respectively, 0.0486, 0.0559, and 0.0270. Moreover, there is large uncertainty in the high-appearing values of S_α^{expt} for the unfavored decays of ^{205}Rn (0.0960 ± 0.0488) and ^{220}At (0.0935 ± 0.0421). These large uncertainties are due to large uncertainties in the released energy value for the decay of ^{205}Rn ($Q_\alpha = 6.390 \pm 0.050$), and in the experimental half-life time and the ground-state spin and parity of the involved nuclei for the decay of ^{220}At, as shown in Table I. In Fig. 3, the extracted preformation probability inside the even-odd isotones of $N = 121,133$ and $N = 157$, and the odd-even isotones of $N = 126$, 130, and 154, in addition to the odd-odd ones of $N = 129$, 131,

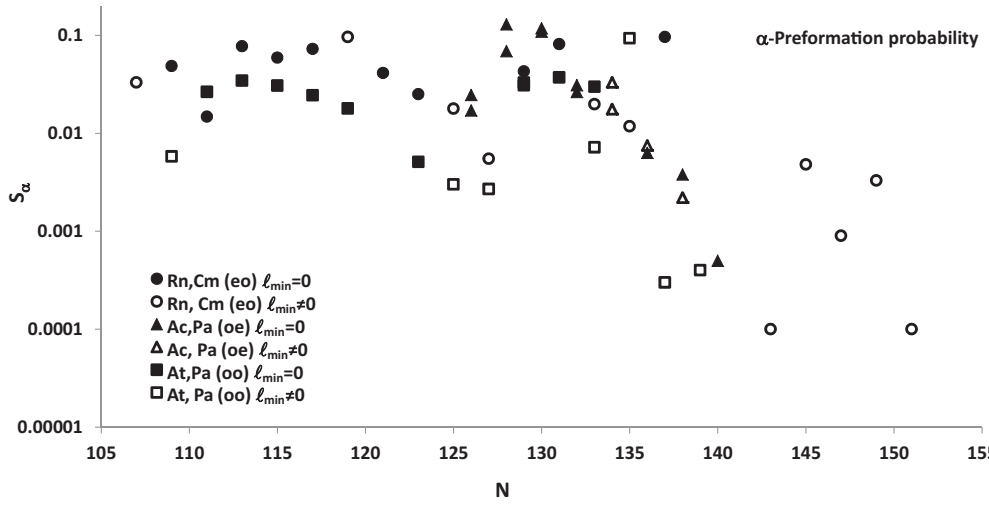

FIG. 2. The estimated α preformation probability [$S_\alpha(T_{1/2}^{\text{expt}})$] inside even ($Z$)—odd ($N$) Rn and Cm isotopes, odd-even Ac and Pa isotopes, and odd-odd At and Pa isotopes versus the neutron number of the parent α emitter. While the open symbols represent unfavored decays with involved transferred angular momentum ($\ell_{\min}$), the solid ones represent favored decays ($\ell_{\min} = 0$) taken from Ref. [9].

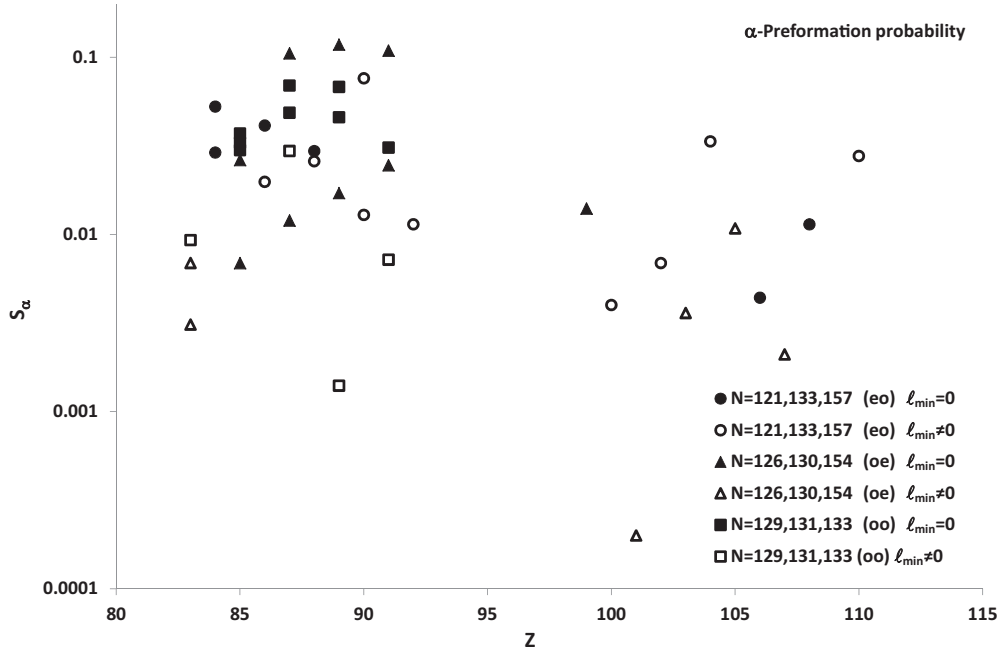

FIG. 3. As Fig. 2 but for the even-odd isotonic chains of $N = 121,133,157$, the odd-even isotonic chains of $N = 126,130,154$, and the odd-odd isotonic chains of $N = 129,131,133$ versus the charge number of the parent α emitters.

and 133 are presented versus the charge number of the α emitters. The results obtained in the present work for the unfavored decays are compared in the same figure with the corresponding values for the favored decays which were obtained in Ref. [9]. For the unfavored decays, the deduced preformation probability inside the odd-even isotones presented in Fig. 3 ranges between 0.0002 ± 0.0001 (^{255}Md) and 0.0108 ± 0.0062 (^{259}Db). Inside the presented even-odd [odd-odd] isotones, the extracted $S_\alpha^{\rm expt}$ has values lying between 0.0040±0.0001 (^{257}Fm) and 0.0761±0.0480 (^{211}Th) [0.0014 (^{220}Ac) and 0.0296 ± 0.0008 (^{220}Fr)]. The corresponding values for the presented favored decays of odd-even, even-odd, and odd-odd nuclei lie between 0.0069 ± 0.0001 (^{211}At) and 0.1180 ± 0.0485 (^{219}Ac), 0.0044 ± 0.0022 (^{263}Sg) and 0.0527 ± 0.0018 (^{217}Po), and 0.0299 ± 0.0069 (^{218}At) and 0.0692 ± 0.0421(^{218}Fr), respectively. In general, the average preformation probability for the displayed unfavored (favored) decays of odd-even, even-odd, and odd-odd nuclei are 0.0045 (0.0481), 0.0242 (0.0280), and 0.0119 (0.0453), respectively. Again, the results presented in Figs. 2 and 3 indicate that the preformation probability tends to decrease if the parent and daughter nuclei have different ground state spins and/or parities. To check this conclusion if the α-decay mode involves excited nuclei, we compare in Table II two decaying modes for each presented α emitter. The first α-decay mode takes place between two ground states. One or two of the participating nuclei in the second α-decay mode are in excited isomeric states. As shown in Table II, for the same decaying nucleus, the preformation probability increases when the formed daughter is in a state

TABLE II. Same as Table I, without the last two columns, but for α-decay modes involving nuclei in isomeric states. The corresponding ground state to ground state decays are listed for comparison. The superscripts m and p indicate assignments to the first and third excited isomeric states, respectively [29]. The uncertainties in the experimental half-life time and the intensity of the decay mode are both considered in the mentioned partial half-lives [29].

Pare.	Dau.	J_P^π	J_D^π	$\ell_{\rm min}$	Q_α (MeV)	$T_{1/2}^{\rm expt}$ (s)	$S_\alpha^{\rm expt}$ [Eq. (1)]
^{185}Pb	^{181}Hg	$3/2^-$	$1/2^{[-]}$	2	6.695 ± 0.005	6.300 ± 0.400	0.0107 ± 0.0011
^{185}Pb^m	^{181}Hg^m	$13/2^+$	$13/2^+$	0	6.555 ± 0.050	11.053 ± 5.827	0.0204 ± 0.0159
^{187}Pb	^{183}Hg	$3/2^-$	$1/2^-$	2	6.393 ± 0.006	$(1.681 \pm 0.386)\times10^2$	0.0057 ± 0.0016
^{187}Pb^m	^{183}Hg^m	$[13/2^+]$	$[13/2^+]$	0	6.208 ± 0.012	$(1.573 \pm 0.287)\times10^2$	0.0186 ± 0.0055
^{186}Bi	^{182}Tl	(3^+)	(7^+)	4	7.757 ± 0.012	$(1.480 \pm 0.070)\times10^{-2}$	0.0167 ± 0.0022
^{186}Bi^m	^{182}Tl^p	(10^-)	10^-	0	7.425 ± 0.120	$(9.800 \pm 0.400)\times10^{-3}$	0.0487 ± 0.0362
^{187}Bi	^{183}Tl	$[9/2^-]$	$1/2^{(+)}$	5	7.779 ± 0.004	0.037 ± 0.002	0.0168 ± 0.0014
^{187}Bi^m	^{183}Tl	$[1/2^+]$	$1/2^{(+)}$	0	7.887 ± 0.011	$(3.700 \pm 0.200)\times10^{-4}$	0.0284 ± 0.0037
^{195}Bi	^{191}Tl	$(9/2^-)$	$(1/2^+)$	5	5.832 ± 0.005	$(1.114 \pm 0.756)\times10^6$	0.0249 ± 0.0178
^{195}Bi^m	^{191}Tl	$(1/2^+)$	$(1/2^+)$	0	6.232 ± 0.008	139.190 ± 36.810	0.0478 ± 0.0161

TABLE III. The fit parameters of the semiempirical expression given by Eq. (14) for the α preformation probability inside 284 favored decays [7,9]. The values of the dimensionless parameters α and β are kept fixed at $\alpha = 0.003$ and $\beta = 0.006$.

Z_0	N_0	Z_c	N_c	A
50	82	8	8	0.110
70	82	6	8	0.067
	102		12	0.062
82	82	12	8	0.073
	102		12	0.078
	126		12	0.105
	150		14	0.087
102	126	14	12	0.108
	150		14	0.103

of the same spin-parity as that of the parent nucleus state. However, this is valid whether the involved nuclei are in their ground states or any of them is in one of its isomeric states.

Now, in the context of our results, we shall modify the semiempirical formula given by Eq. (13) to account for the hindrance in the preformation probability in the unfavored decays, with respect to the favored ones. We suggest that the modified expression reads

$$S_\alpha = \frac{A e^{-\alpha(Z-Z_0-Z_c)^2} e^{-\beta(N-N_0-N_c)^2} - a_p}{a_\ell}. \quad (14)$$

Here, the coefficient a_ℓ is introduced to account for the difference between the ground state spin and/or parity of the participating nuclei. However, for favored decays, $a_\ell = 1$. Our next step is to do two things. First, we try to reduce the number of fit parameters of Eq. (14) by fixing some of its variable parameters given in Refs. [7,9]. Second, we look into the form of a_ℓ. By optimizing the fit to the results of 284 even-even, odd-A, and odd-odd favored decays given in Refs. [7,9] and keeping fixed values of $\alpha = 0.003$ and $\beta = 0.006$, we obtain the parametrization of Eq. (14) listed in Table III. The pairing term (a_p) is still given by Eq. (13). With respect to the experimental half-life times of the mentioned 284 favored decays, taking account of the experimental errors, the standard deviation of their calculated half-lives based on the parametrization of S_α [Eq. (13)] given in Table III is $\sigma = 0.375$. The standard deviation is given as, $\sigma = \sqrt{\sum_{i=1}^{n} [\log_{10}(T_{1/2}^{\rm calc}/T_{1/2}^{\rm expt})]^2/(n-1)}$. Based on the present results of $S_\alpha^{\rm expt}$ for the studied 161 unfavored decays, the adopted a_ℓ coefficient is given in terms of the mass number of the parent nucleus (A) and the minimum allowed value of the transferred angular momentum ($\ell_{\rm min}$) as

$$a_\ell = \frac{A^2}{3190\sqrt{\ell_{\rm min}}} - 3.9. \quad (15)$$

Figure 4 shows the extracted preformation probability based on the experimental half-life time, Eq. (1), and that estimated by the empirical formula given by Eq. (14), for the odd-odd isotopes of Bi ($Z = 83$), the odd-even isotopes of Np ($Z = 93$), and the even-odd isotopes of Ds ($Z = 110$). The differences between the thick curves [Eq. (14) with a_ℓ] and the thin ones [Eq. (14) without a_ℓ] represent the hindrance in the preformation probability due to the inclusion of the angular momentum term a_ℓ. Considering this hindrance in preformation probability, due to the difference in the ground state spin-parity of the involved nuclei, the standard deviation of the half-life times calculated using S_α [Eq. (14)] improves substantially from $\sigma = 1.137$ (without a_ℓ) to $\sigma = 0.723$. The calculated half-lives of ^{236}Np ($S_\alpha^{\rm expt} = 0.0001 \pm 0.0001$), ^{244}Bk ($S_\alpha^{\rm exp\,t} = 0.00001 \pm 0.00001$), and ^{228}Pa ($S_\alpha^{\rm expt} = 0.0003$) yield the largest deviations from the experimental ones. Actually, in addition to the low extracted preformation probability inside these three decays, they are characterized by an α-decay mode of low intensity [29]. Moreover, the available experimental half-lives and intensities of these decays are a little old [29,38,39]. If we exclude these three decays, the obtained standard deviation becomes $\sigma = 0.664$. For all mentioned 445 decays, the total standard deviation of the calculated half-life times, based on the preformation probability given by Eq. (14), from the experimental values is $\sigma = 0.529$.

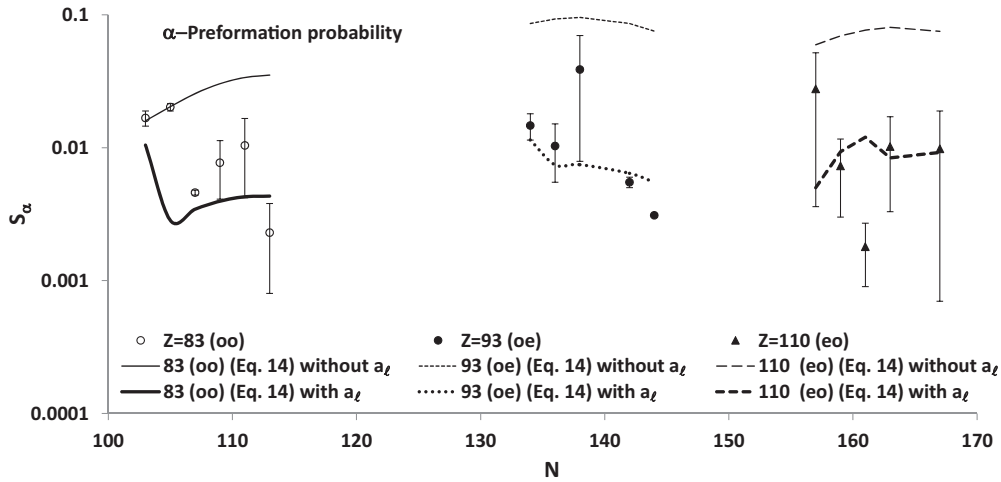

FIG. 4. Comparison of the α-preformation probability inside the odd-odd isotopes of Bi, the odd-even isotopes of Np, and the even-odd isotopes of Ds as extracted from the experimental half-life time, Table I, and its values deduced using, Eq. (14), with and without the angular momentum coefficient (a_ℓ).

To examine the ability of our model to predict information on the ground state spin-parity of the involved nuclei, we will consider the α decay of ^{215}U ($T_{1/2} = 0.730^{+1.33}_{-0.29}$ ms and $E_\alpha = 8.428 \pm 0.030$ MeV) which was observed recently [40]. Considering transferred angular momentum values of $\ell = 0$, 1, 2, and 3, the calculated decay width and the preformation probability [Eq. (14)] yield half-life times of $3.345^{+0.775}_{-0.638}$ ms, $43.022^{+10.124}_{-8.172}$ ms, $39.668^{+8.751}_{-7.864}$ ms, and $50.810^{+11.592}_{-9.966}$ ms, respectively. As seen, the closest obtained value to the experimental half-life time is the one corresponding to $\ell = 0$. However, our calculations strengthen the $\ell = 0$ assignment that was proposed tentatively for this decay in Ref. [40]. This suggests that the ^{215}U nucleus has a typical ground state spin-parity like that assigned for ^{211}Th, from trends in neighboring nuclides, which is $5/2^-$ [29].

IV. SUMMARY AND CONCLUSION

We studied the ground state to ground state unfavored decays of 161 odd (Z)—even (N), even-odd, and odd-odd open-shell nuclei. We investigated the preformation probability inside these nuclei. We also explored the role of the transferred angular momentum transferred by the emitted α particle in the different physical quantities involved in the unfavored decay process. The detailed calculations showed that the angular momentum of the emitted α particle increases the assault frequency where it decreases the width of the internal pocket of the interaction potential, shifting its lowest point up. Conversely but more effectively, it reduces the penetration probability because it produces a higher Coulomb barrier with a larger barrier width. The net effect appears as hindrance in the decay width. Consequently, the half-life increases substantially for the unfavored decays. Most importantly, we found that for a parent with a given ground state spin-parity, the probability of forming an α cluster and a daughter nucleus with different ground state spin and/or parity is less than if the daughter nucleus has the same spin and parity of parent. The formula relating the α preformation probability to the numbers of protons and neutrons outside the closed shells in the parent nuclei is modified to take account of the hindrance in the preformation probability associated with the unfavored decays between ground states.

[1] S. Peltonen, D. S. Delion, and J. Suhonen, Phys. Rev. C **75**, 054301 (2007).
[2] M. Bhattacharya, S. Roy, and G. Gangopadhyay, Phys. Lett. B **665**, 182 (2008).
[3] W. M. Seif, M. Shalaby, and M. F. Alrakshy, Phys. Rev. C **84**, 064608 (2011).
[4] R. G. Lovas, R. J. Liotta, A. Insolia, K. Varga, and D. S. Delion, Phys. Rep. **294**, 265 (1998).
[5] J. C. Pei, F. R. Xu, Z. J. Lin, and E. G. Zhao, Phys. Rev. C **76**, 044326 (2007).
[6] A. N. Andreyev *et al.*., Phys. Rev. Lett. **110**, 242502 (2013).
[7] W. M. Seif, J. Phys. G: Nucl. Part. Phys. **40**, 105102 (2013).
[8] M. Ismail and A. Adel, Phys. Rev. C **88**, 054604 (2013).
[9] W. M. Seif, Phys. Rev. C **91**, 014322 (2015).
[10] S. M. S. Ahmed, R. Yahaya, S. Radiman, and M. S. Yasir, J. Phys. G: Nucl. Part. Phys. **40**, 065105 (2013).
[11] D. E. Ward, B. G. Carlsson, and S. Åberg, Phys. Rev. C **88**, 064316 (2013).
[12] P. Mohr, Phys. Rev. C **73**, 031301(R) (2006); **61**, 045802 (2000).
[13] Jianmin Dong, Hongfei Zhang, Yanzhao Wang, Wei Zuo, and Junqing Li, Nucl. Phys. A **832**, 198 (2010).
[14] Dongdong Ni and Zhongzhou Ren, Phys. Rev. C **82**, 024311 (2010).
[15] S. S. Malik and R. K. Gupta, Phys. Rev. C **39**, 1992 (1989)
[16] B. Buck, A. C. Merchant, and S. M. Perez, Phys. Rev. C **45**, 2247 (1992).
[17] M. Wang, G. Audi, A. H. Wapstra, F.G. Kondev, M. MacCormick, X. Xu, and B. Pfeiffer, Chin. Phys. C **36**, 1603 (2012).
[18] F. L. Stancu and D. M. Brink, Nucl. Phys. A **270**, 236 (1976).
[19] M. Brack, C. Guet, and H.-B. Håkansson, Phys. Rep. **123**, 275 (1985).
[20] V. Yu. Denisov and W. Noerenberg, Eur. Phys. J. A **15**, 375 (2002).
[21] W. M. Seif, Eur. Phys. J. A **38**, 85 (2008).
[22] P. Möller, J. R. Nix, W. D. Myers, and W. J. Swiatecki, At. Data Nucl. Data Tables **59**, 185 (1995).
[23] E. Chabanat, E. Bonche, E. Haensel, J. Meyer, and R. Schaeffer, Nucl. Phys. A **635**, 231 (1998).
[24] B. Buck, J. C. Johnston, A. C. Merchant, and S. M. Perez, Phys. Rev. C **53**, 2841 (1996).
[25] Chang Xu and Zhongzhou Ren, Phys. Rev. C **73**, 041301(R) (2006).
[26] J. W. Negele and D. Vautherin, Phys. Rev. C **5**, 1472 (1972).
[27] M. Ismail and W. M. Seif, Phys. Rev. C **81**, 034607 (2010).
[28] M. Ismail, W. M. Seif, A. Y. Ellithi and F. Salah, J. Phys. G **35**, 075101 (2008).
[29] G. Audi, F. G. Kondev, M. Wang, B. Pfeiffer, X. Sun, J. Blachot, and M. MacCormick, Chin. Phys. C **36**, 1157 (2012).
[30] M. S. Basunia, Nucl. Data Sheets **108**, 633 (2007).
[31] A. N. Andreyev *et al.*, J. Phys. G: Nucl. Part. Phys. **37**, 035102 (2010).
[32] E. Browne and J. K. Tuli, Nucl. Data Sheets **114**, 751 (2013).
[33] Khalifeh Abusaleem, Nucl. Data Sheets **112**, 2129 (2011).
[34] N. Nica, Nucl. Data Sheets **106**, 813 (2005).
[35] E. Browne and J. K. Tuli, Nucl. Data Sheets **114**, 1041 (2013).
[36] J. Dvorak *et al.*, Phys. Rev. Lett. **100**, 132503 (2008).
[37] M. Ismail, W. M. Seif, and H. El-Gebaly, Phys. Lett. B **563**, 53 (2003).
[38] E. Browne and J. K. Tuli, Nucl. Data Sheets **107**, 2649 (2006).
[39] Balraj Singh and E. Browne, Nucl. Data Sheets **109**, 2439 (2008).
[40] H. B. Yang *et al.*, Eur. Phys. J. A **51**, 88 (2015).